İSTANBUL UNIVERSITY CERRAHPAŞA

ORIGINAL ARTICLE
Electrica 2023; 23(3): 475-491

Fault Analysis of Power System Transient Stability with Thyristor-Controlled Series Capacitor Controller Model Using Flower Pollination Algorithm for Its Parameters

Ghamgeen Izat Rashed[1], Duku Otuo-Acheampong[1], Akwasi Amoh Mensah, Hussain Haider[1]

[1]School of Electrical Engineering and Automation, Wuhan University, Wuhan, China
[2]Automation Science and Engineering and Automation, South China University of Technology, Guangzhou, China

Cite this article as: G. Izat Rashed, D. Otuo-Acheampong, A. Amoh Mensah and H. Haider, "Fault analysis of power system transient stability with thyristor-controlled series capacitor controller model using flower pollination algorithm for its parameters," *Electrica*, 23(3), 475-491, 2023.

ABSTRACT

This paper proposed the dynamic security assessment for the transient stability using thyristor-controlled series capacitor (TCSC) controller. The stability criteria are based on the severity indices for analyzing the fault on the power system. The index uses time-domain analysis simulation, which makes it easier and simpler to implement. The optimal location and parameter setting of the TCSC is formulated as an optimization problem solved by using the flower pollination algorithm (FPA) due to its higher convergence rate. The proposed index is tested on the modified IEEE 14-bus and IEEE 68-bus, large-scale system. The effects of a three-phase short-circuit fault, different fault locations, and fault clearing method are then further discussed. An analysis is done to determine how the faults on lines affect the transient stability of the load and generator bus in the system. The findings show that by employing the TCSC lead–lag controller using the FPA for tuning, the voltage drop was improved and stability margins were greatly increased with damping out transient power oscillation. To demonstrate the effectiveness of using the proposed FPA to solve the suggested problem, the results are also compared with that of artificial bee colony to prove its robustness.
***Index Terms*—**Flower pollination algorithm, severity indices, thyristor-controlled series capacitor, transient voltage stability.

I. INTRODUCTION

Modern power systems experience challenges during their operation, such as operating closer to their stability limits [1]. The need to keep the power systems secure under demanding operating conditions has become critical due to high power consumption, population growth, and advances in technology. The electrical power network is designed to provide uninterrupted power supply, but the way unpredictable incidents can happen on the network during the process of generation, transmission, or distribution can hinder the quality of power supply, making the system unstable sometimes. This raises concerns about the reliability, risk, and security of electricity [2]. Such incidence can be all kinds of faults, i.e., short-circuit, open-circuit, or three-phase faults. A situation like this causes serious issues in the daily lives of millions of people, including economic loss such as closure of industries and factories and other consequences. It is the mandate of the power operators to ensure that the power system is always running stable.

Power system stability is the capacity of a power system to maintain an operating equilibrium under normal operating conditions and to return to an acceptable state of equilibrium following a disturbance [3]. These disturbances may happen by the abrupt removal of the load or line and an unexpected line failure. If the fault develops and is not fixed within a predetermined time frame, it could result in severe damages to the system, resulting in a blackout or power loss. This research is mainly focused on transient stability, which is referred to as the ability of the system to return to its normal conditions after being subjected to large or serious disturbances [4].

Transient stability has always been a critical and key issue for modern power system analysis and control for ensuring safe operation [5]. It is influenced by a number of factors, including network structure, fault type, and location [6]. There are two types of faults which are shunt fault and series fault [7]. Open-circuit faults are classified as series fault, while short-circuit faults as shunt faults. This manuscript deals with shunt faults because they have a greater impact on system

Corresponding author:
Ghamgeen Izat Rashed

E-mail:
ghamgeen@whu.edu.cn

Received: October 21, 2022

Accepted: January 11, 2023

Publication Date: March 29, 2023

DOI: 10.5152/electr.2023.22201

stability and reliability. Studies have shown that three-phase short-circuit fault is the severest of all faults in power systems. Occurrence on the transmission line will cause severe voltage drop on the system from a distance, which is not easy to identify and that is hard to recover from, which could also lead to total blackout. Performing a simulation on the transmission line also finds that the transient voltage stability issue will get even worse when drastic measures are not taken to correct the problem. Under normal circumstances, the system must quickly disconnect that specific line from the power system when it encounters a short-circuit fault. However, cutting off that line could result in an overload of another line, so clearing the fault as soon as possible is crucial for the continued operation of power systems. Numerous factors often lead to the analysis of three-phase short-circuit faults, such as preventing voltage collapse of the power system and determining the correct rating of the protective device such as the circuit breakers and switchgear. The focus will be on the power system's transmission system since short-circuit faults on this system cause generation plants to lose synchronism and result in significant blackouts of the power system.

Basically, there are two different kinds of transient stability assessment (TSA) methods: the time-domain simulation [8-10] and the direct method [11, 12]. These techniques typically have more than just determining whether the system will be stable after a disturbance. Although they are faster in terms of speed, they come with a lot of constraints when modeling [13, 14]. The time-domain method is adopted in this research because of its accuracy that comes with a detail description and the capability of handling any modeling of the power system; however, its calculation speed is very slow, which needs to be improved [15, 16]. Several stability indices have been used in numerous research works for the assessment of stability of large power systems such as transient security indices [17], small signal stability index [18], rotor angle stability index [19], frequency stability index [20], and transient voltage stability index . The TSA approach is the mostly used method for the analysis of faults on the power system because it provides details of the dynamic behavior of the system components. In [21], the TSA approach is proposed by using a random vector functional link network which is optimized by the Jaya algorithm to assess the transient stability of the power system. The TSA approach was introduced in [22] by using the transient severity index for two purposes: first to categorize the generators in coherent groups and second to rank them according to the severity level which was very effective when applied on the IEEE system.

Recent grid upgrades include the installation of flexible AC transmission system (FACTS) devices to improve power transfer limits, improve system damping, and increase transient voltage stability, all of which ensure that the power system operates safely and efficiently [23, 24]. But the question is how to locate the optimal place and rating of this device to be installed in order to help clear the fault quickly is quite a challenge. The current research and developments in power electronics have paved the way for the use of FACTS devices that are dependable and of high speed such as static VAR compensator, STATCOM, unified power flow controller (UPFC), and thyristor-controlled series capacitor (TCSC) to be used for transient stability with the tuning of its parameters being developed as an optimization problem to be solved using intelligent techniques like the harmony search algorithm, quasi-oppositional harmony search (QOHS) algorithm, and genetic algorithm (GA). Thyristor-controlled series capacitor has been given much attention due to the benefits it offers, and it has been used with different controller designs. As a result, the FACTS device that will be employed in this research is the TCSC. Some of such recent research are discussed.

Nandi et al. [17] proposed the QOHS technique for the design of Proportional-Integral-Derivative controller (PID) and TCSC controller gains, and the results of the research work justify why the proposed QOHS–TCSC–PID is a better damping controller than the other controller types that were compared. In [25], an Static Synchronous Series Compensator (SSSC)-based wide-area controller is designed to improve the power system stability, and its setting and tuning are optimized using a GA based on the integral time error criteria and implemented with the consideration of time delay which was modeled using the Pade approximation method. A comparative analysis between two controllers was studied [26], which was done by the design and implementation of proportional integral (PI)-controlled (STATCOM) controllers and fuzzy logic-controlled STATCOM controllers with different fault conditions. In [27], power system stabilizer and FACTS damping controllers were used to stabilize a large-scale power system with the implementation of improved planted growth simulation algorithm for the controller's parameters. Meziane et al. [28] proposed the PI derivative controller with TCSC to improve the dynamic stability of the system. With that approach, the controller gain was tuned using the interval type-2 fuzzy logic. The use of the UPFC to improve the transient stability of power systems was studied in [29], in which the author proposed a non-linear technique as the control scheme for the device that is based on transient energy function and improved two-order sliding mode observer. A synergetic control theory method studied in [30] was applied for the design of a decentralized TCSC controller for the analysis of transient stability. In [31], the control parameters of the robust wide-area damping controller for the TCSC were solved by using the linear matrix inequality approach for damping enhancement which was superior when compared to the H controller.

Of all the controllers discussed, the use of the conventional lead–lag controller for the TCSC is now widely used due to the advantages it provides for the effective power oscillation damping of the system and enhancement of the transient stability [32]. Most of the studies about using FACTS devices only placed the device at the higher load buses. This method mostly does not give a good result by improving the stability of the system. Therefore, determining the optimal location and parameters of the FACTS device controller model using a meta-heuristic approach can guarantee a successful voltage drop enhancement at the bus.

This paper proposes the DSA-based TSA using the severity indices for the simulation and analysis to identify the transient voltage stability weakness when a three-phase short-circuit fault occurs on the transmission lines with and without a TCSC controller. The novelty of this research is the optimal location and parameter tuning of the TCSC lead–lag controller using the flower pollination algorithm (FPA) based on the integral of time-weighted absolute error (ITAE) as the objective function to improve the transient stability of the power system, subjected to severe disturbances. Artificial bee colony (ABC)-based parameter tuning results are compared to that of the proposed FPA-based parameter tuning of the devices to assess its effectiveness.

The paper is organized as follows: Section II describes the proposed method. Section III describes the TCSC model and its controller. Section IV explains the FPA and its implementation. Section IV presents the case system that will be used to verify the proposed

approach. Section V discusses the results and discussion, and finally, Section VI concludes the paper.

II. PROPOSED METHOD

The severity indices using the time-domain simulation is proposed to determine the transient stability of the system. If the power system experiences a significant disturbance, the algebraic variables change instantly, while the dynamic variables could take some time before their state values change, according to the differential algebraic equations represented in . After the disturbances have cleared, it is anticipated that the variables will either return to their original operating state or attain new, acceptable steady-state operating values, but this is not always the case.

The dynamic equation of the power system is expressed as follows:

$$\dot{x} = f(\boldsymbol{x}, \boldsymbol{y}, \lambda) \tag{1}$$

$$0 = g(\boldsymbol{x}, \boldsymbol{y}, \lambda) \tag{2}$$

where $\boldsymbol{x}$ is a vector representing state variables like the speed and angle of the rotors, $\boldsymbol{y}$ is the vector of algebraic variables such as voltages, and λ is the vector of model parameters such as generation levels, load levels, and transmission line impedances.

The dynamic response to a disturbance of a state variable linked to a machine is shown in Fig. 1.

The three-phase short-circuit fault occurred at time t_1 and was cleared at t_2. The deviation from the initial steady-state operating point $x(t_0)$ can be used to determine the fault's severity at any time t. The severity index is the weighted sum of squares of error defined as in –:

$$SI(t) = \frac{1}{m}\sum_{i=1}^{m}\sum_{j=1}^{k} w_{i,j}\left(x_{i,j}(t) - x_{i,j}(t_0)\right)^2 \tag{3}$$

$$SI(t) = \frac{1}{m}\int_0^{\infty}\sum_{i=1}^{m}\sum_{j=1}^{k} w_{i,j}\left(x_{i,j}(t) - x_{i,j}(t_0)\right)^2 dt \tag{4}$$

$$\sum_{j=1}^{k} w_{i,j} = 1 \tag{5}$$

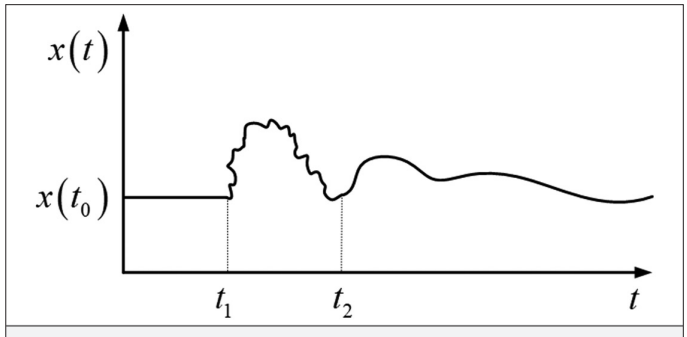

Fig. 1. Dynamic response of a machine state variable. The oscillation between t_1 and t_2 means a large disturbance happened at t_1 and lasted till it was cleared at t_2. During the post-fault period, the system was stable.

$$w_{1,j} = w_{2,j} = w_{3,j} = \ldots = w_{m,j} \forall j \tag{6}$$

where W_j is the weight associated with the state variable $x_{i,j}$. M is the number of machines and k is the number of the state variables.

III. THYRISTOR-CONTROLLED SERIES CAPACITOR MODEL AND ITS CONTROLLER

The type of device used in this paper is TCSC, which is classified as one of the most important controllers with its configuration shown in Fig. 2. The TCSC is a series-connected device that adjusts the line impedance by connecting a variable reactance in series with the line, thereby regulating the power flow across the line and decreasing the reactive power loss [6, 33, 34]. The static model of TCSC connected between branches (a and b) is presented in Fig. 3. Connecting in series helps to increase the dynamic stability of power transmission systems. The conventional dynamic model-based damping controller of the TCSC is shown in Fig. 4.

The thyristor firing angle (α) has two functional areas: one is the capacitive area $X_{TCSC}(\alpha) < 0$, where $\alpha_{C,lim} < \alpha < 180$ and the other is the inductive area $X_{TCSC}(\alpha) > 0$, where $90 < \alpha < \alpha_{L,lim}$ [13]. In line with a system control algorithm, the firing angles of the thyristors are adjusted to change the TCSC reactance, often in response to some system parameter [35]. So, the TCSC is modeled in this study as a variable capacitive reactance so that it can generate reactive power to the system for stability reason. The equivalent TCSC reactance for the relationship between conduction angle (σ) ($\sigma = \pi - \alpha$) and the TCSC reactance $X_{TCSC}(\sigma)$ in the steady state are defined as follows [1]:

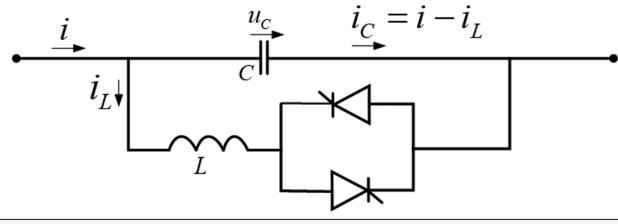

Fig. 2. Schematic diagram of a thyristor-controlled series capacitor. This device configuration consists of three main components: bypass inductor (L), capacitor banks (C), and two antiparallel thyristor T1 and T2.

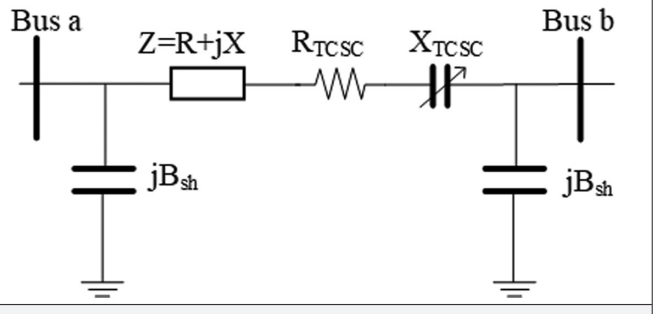

Fig. 3. Transmission line model with a thyristor-controlled series capacitor (TCSC). This shows the transmission line model represented by lumped π-equivalent parameters with a TCSC linked between bus a and bus b. The TCSC changes the line impedance during the load flow due to series capacitance.

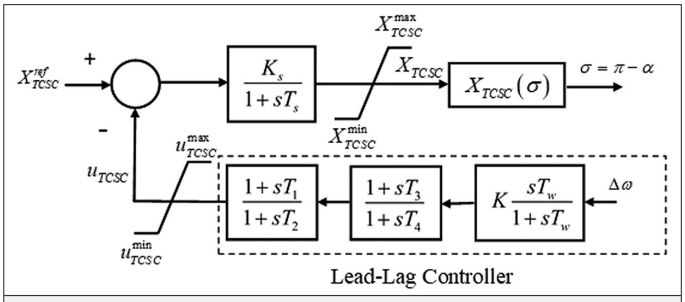

Fig. 4. Block diagram of thyristor-controlled series capacitor (TCSC) with a lead–lag controller model. This consists of a gain block, a signal washout, and a two-stage phase compensation block.

$$X_{TCSC}(\sigma) = X_C - \frac{X_C^2}{(X_C - X_P)}\frac{\sigma + \sin\sigma}{\pi} + \frac{4X_C^2}{(X_C - X_P)}\frac{\cos^2(\sigma/2)}{(k^2-1)}\frac{\left(k\tan(k\sigma/2) - \tan(\sigma/2)\right)}{\pi} \quad (7)$$

where X_C is the nominal reactance of the fixed capacitor C, X_P is the inductive reactance of inductor L connected in parallel with a fixed capacitor, and k is the compensation ratio.

From the controller model in Fig. 4, the input signal is the speed deviation $\Delta\omega$, and the output signal is the reactance $X_{TCSC}(\sigma)$. It consists of a gain block, a signal washout, and two-stage phase compensation block. The transfer function of the TCSC controller is:

$$u = K_P\left(\frac{sT_w}{1+sT_w}\right)\left(\frac{1+sT_1}{1+sT_2}\right)\left(\frac{1+sT_3}{1+sT_4}\right)y \quad (8)$$

where u and y are the TCSC controller output and input signals, respectively.

The lead–lag controller parameters are tuned based on the ITAE using the FPA. This is proposed for the controller for reducing the steady-state output error after disturbances and effectively suppressing low-frequency oscillation in power systems [36]. It is defined as a minimization function expressed as follows:

$M = \int_0^{ti} t\left|e(t)\right|dt$ where "e" is the error signal and t_1 is the time range of simulation.

IV. FLOWER POLLINATION ALGORITHM

The FPA, a meta-heuristic search algorithm developed by Xin-She Yang, was modeled after the pollination procedure of flowering plants [37]. The following four rules are used for the implementation:

1. In the global pollination process, biotic and cross-pollination are considered, and pollen-carrying pollinators obey Lévy flight [38].
2. Abiotic pollination and self-pollination are methods used for local pollination.
3. Pollinators such as insects develop flower constancy, which is equivalent to reproduction probability, and it is proportional to the similarity of two flowers involved.
4. A switch probability, $p \in [0,1]$, is used to control the interaction of local and global pollination.

These rules have to be converted into proper updating equations. The global pollination step and flower constancy step can be represented by:

$$x_i^{t+1} = x_i^t + \gamma L(\lambda)\left(g_* - x_i^t\right) \quad (9)$$

where x_i^{t+1} is the solution vector x_i at iteration t, g_* is the current best solution found among all solutions at the current iteration, γ is a scaling factor, and $L(\lambda)$ is a step-size parameter.

The parameter L is the strength of pollination, and it represents a Levy distribution that is given by:

$$L\Gamma: \frac{\lambda\Gamma(\lambda)\sin(\pi\lambda/2)}{\pi}\frac{1}{s^{1+\lambda}}, \left(s\,?\,s_0 > 0\right) \quad (10)$$

where $\Gamma(\lambda)$ is the standard gamma function. Rules 2 and 3 can both be modeled as follows for the local pollination:

$$x_i^{t+1} = x_i^t + \varepsilon\left(x_j^t - x_k^t\right) \quad (11)$$

where x_j^t and x_k^t are pollen from different flowers of the same plant species and ε is a random number between 0 and 1.

A. Flower Pollination Algorithm Implementation

In this optimization problem, using the TCSC to inject reactive power into the system to improve the transient stability, the locations and size of the TCSC are the control variables. The flowering species of the algorithm will solve these control variables. To determine the system losses, the control variables for each flower and the load flow are run. The fitness of the flower is determined by the reactive power loss of the load flow. The flower that meets the TCSC placement and parameter requirements and offers the best fitness (the least or smallest loss) is chosen as the global best flower. Two parameters are to be set for this algorithm: the population size ($n = 25$) and the probability switch ($p = 0.8$) [38].

The steps of the FPA algorithm are as follows:

Step 1: Read the system's line and bus data and use the Newton–Raphson for the load flow calculation.
Step 2: Initialize the population size and probability switch $p = 0.8$, $n = 25$.
Step 3: Randomly generate the population of TCSC sizes and locations.
Step 4: Determine the reactive power loss for the generated population by performing load flow.
Step 5: Select the TCSC value with the lowest loss and its location as the current best solution.
Step 6: Verify if the selected branch is attached to the slack bus or the generator. If yes, proceed to step 3; otherwise, go to the next step.
Step 7: Generate new local and global solutions based on p using and .
Step 8: Determine the losses for the updated population by performing load flow.
Step 9: If the obtained losses are smaller than the current best solution, replace it with the updated values. If not, return to step 8.

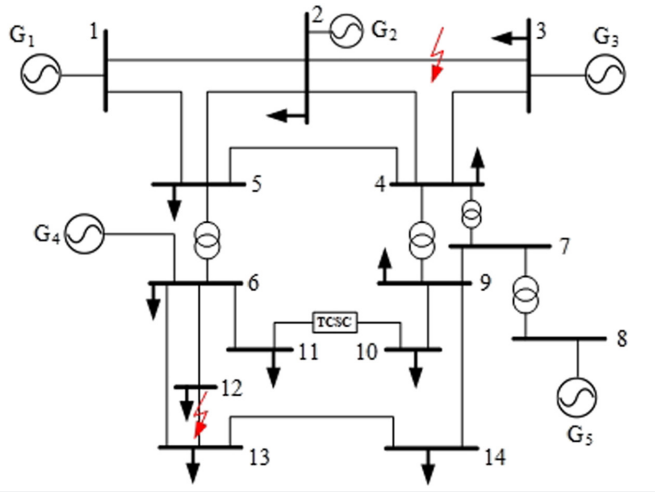

Fig. 5. IEEE 14-bus system with a thyristor-controlled series capacitor (TCSC). The red line in the figure shows the fault's location, one between the generator buses and the other between load buses, with the TCSC located between branches 10 and 11.

Step 10: Print the results if the maximum number of iterations has been reached.

V. CASE SYSTEM

The proposed method is tested on two test systems, including the IEEE 14-bus system and IEEE 68-bus system, as shown in Fig. 5 and Fig. 6. The IEEE 14-bus system is a modified test system for the transient stability having 16 transmission lines, 14 buses, 5 generators, and 4 transformers. Bus 1 is considered as the slack bus during simulations. Also, the IEEE 68-bus system consists of 16 generators, 15 transformers, 68 buses, and 70 transmission lines with bus 65 as the slack bus. The TCSC lead–lag compensator parameter tuning and optimal location are optimized by the FPA algorithm using MATLAB which is integrated into the Neplan software for the analysis and validation of the simulation results on a desktop PC platform outfitted with an Intel(R) Core (TM) i7-4790 CPU @ 3.60GHz, 3.60GHz, and 8 GB RAM.

VI. RESULTS AND DISCUSSION

For the purpose of validating the proposed fault model, a three-phase short-circuit fault on two different transmission lines will be simulated to examine the impact on the power system. On a number of lines, the fault locations are chosen at random, with one fault occurring between generator buses and the other between load buses with different fault distances from the line, which are grouped in two cases. For the assessment, the bus voltage magnitude is used as a reference. The FPA provides the location of a TCSC controller to be between buses 10 and 11 for the modified IEEE 14-bus system and between buses 8 and 9 for the modified IEEE 68-bus system. The total simulation time is 10 s with a sample time of 0.04 s. The proposed FPA-tuned controller simulation is compared with the ABC-tuned controller in all simulations.

A. IEEE 14-Bus System

1) Case A

A three-phase short-circuit fault was applied at line L02–03, which is located between generator bus 2 and generator bus 3. Fig. 7 and Fig. 8 show that the distance of the line fault from bus 2 is 0.1 pu. The faults occurred at $t = 0.5$ s and lasted for 0.5 s. At $t = 1.0$ s, the fault was cleared by two different modes. As shown in Fig. 7, bus 4 suffered the worst voltage magnitude because it was very closer to the line fault so that will be used for the comparison. The voltage decreases from 1.00 p.u. during the pre-fault stage to 0.004 p.u. during the occurrence of the fault from 0.5 s to 1.0 s. The fault was clear by removing the short-circuit fault from the system as shown

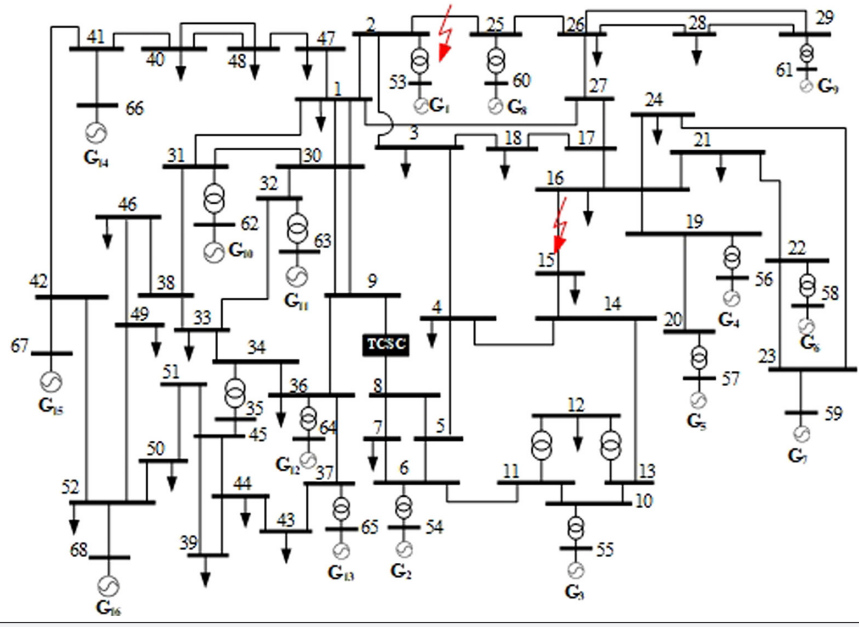

Fig. 6. IEEE 68-bus system with a thyristor-controlled series capacitor (TCSC). The red line in the figure shows the fault's location, one between the generator buses and the other between load buses, with the TCSC located between branches 8 and 9.

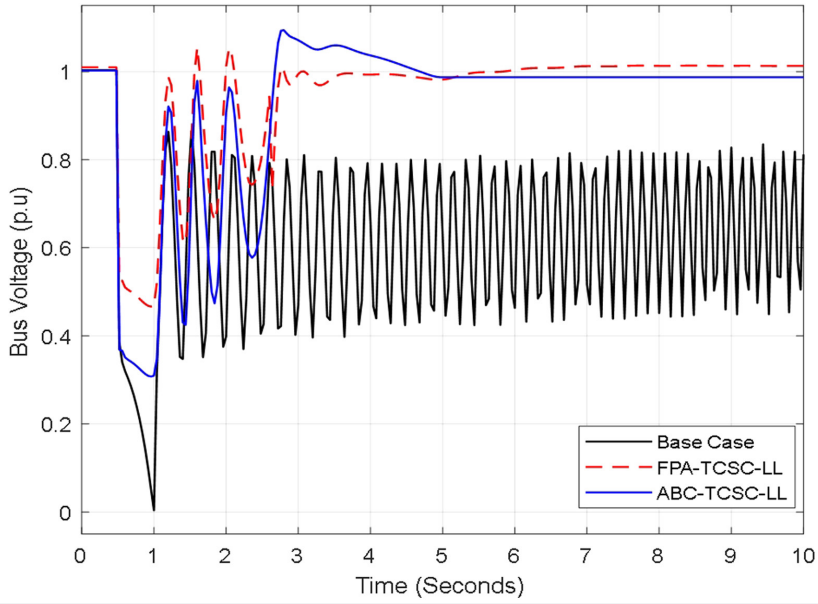

Fig. 7. Voltage magnitude after line fault (L02–03) at 10% distance with/without thyristor-controlled series capacitor (TCSC). The plot consists of three lines: the black line shows the plot of the original system, while the blue line shows the ABC–TCSC controller; the red line shows the system with the proposed flower pollination algorithm (FPA) –TCSC controller injection. The proposed FPA–TCSC controller stabilized the system after the fault was cleared.

in Fig. 7. During the post-fault stage, from $t = 1.0$ s to $t = 10.0$ s, it can be observed that the transient of the system shows that the system is having higher oscillation damping, making it unstable. By using the proposed FPA–TCSC controller to the system enhances the voltage drop from 0.004 p.u. to 0.467 p.u. during the fault stage and quickly suppressed the oscillation, making the system stable after the fault clearance as compared to the ABC–TCSC controller, although it was able to improve the oscillation when also compared to the base case.

Fig. 8 represents the simulation after completely removing the fault branch at both sides of the bus when the fault was cleared. Pre-fault and post-fault stages share the same features as shown in Fig. 7. After clearing the fault, the base case was still unstable with wide

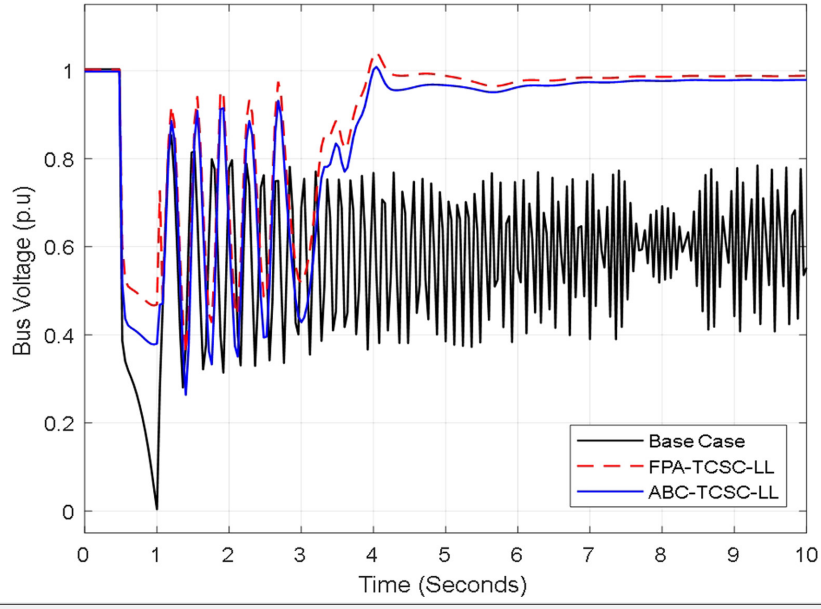

Fig. 8. Voltage magnitude after line fault (L02–03) at 10% distance with/without a thyristor-controlled series capacitor (TCSC) controller. With this graph, the fault was cleared by completely removing the branches from the end. Oscillation was still high in the base case shown in black, but using the proposed flower pollination algorithm (FPA)–TCSC controller made the system stable shown in red line.

oscillation which ends with error; the use of the ABC–TCSC controller damped the oscillation and made it stable, but this took a longer time at around 5.8 s which was almost the same to that obtained with the proposed FPA–TCSC controller which achieved stability at 0.9 p.u.

Both in Fig. 9 and Fig. 10, the fault is located at the midpoint of the line 02–03 that is 50% of the fault location, with bus 4 suffering the most voltage drop of 0.21 p.u. In Fig. 9, at $t = 0$ s before the occurrence of the fault with and without the TCSC controller, the voltage magnitude of all buses was stable, ranging from 1.00 to 1.10 p.u.

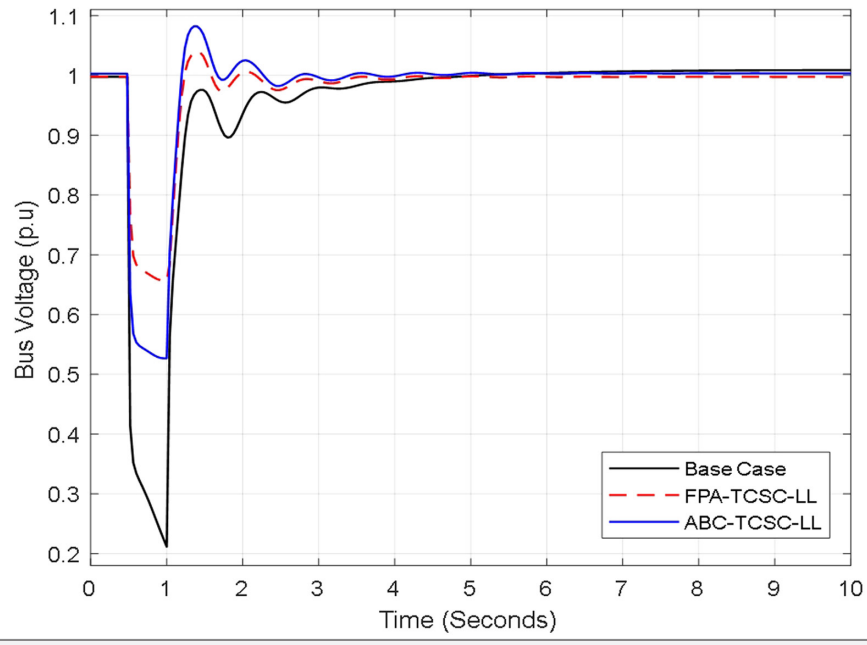

Fig. 9. Voltage magnitude after line fault (L02–03) at 50% distance with/without a thyristor-controlled series capacitor (TCSC) controller. Location of the fault was set at the midpoint of the line fault for the analysis. Using the proposed flower pollination algorithm (FPA)–TCSC controller, as shown in the red line, improved the voltage drop after the fault was cleared by removing the short-circuit fault compared to the base case shown in black color.

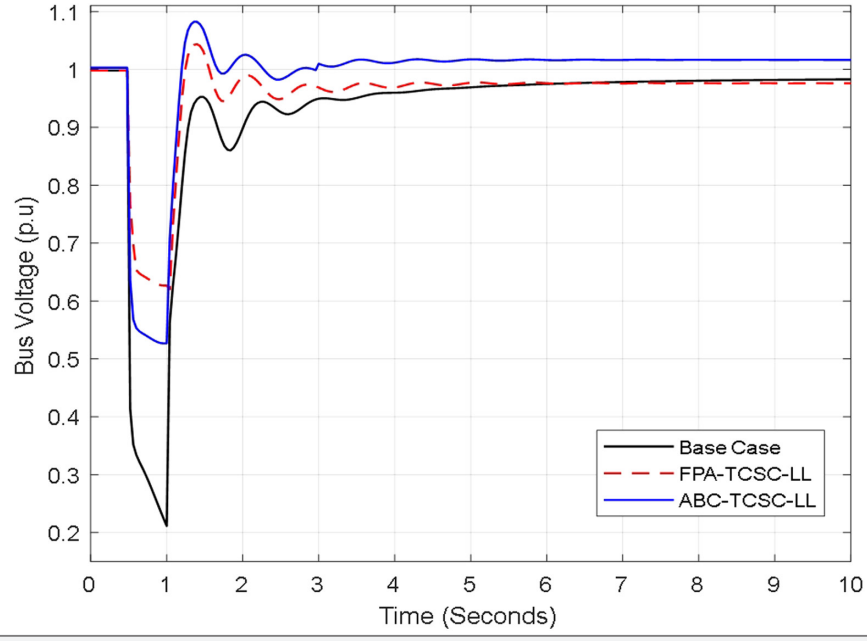

Fig. 10. Voltage magnitude after line fault (L02–03) at 50% distance with/without a thyristor-controlled series capacitor (TCSC) controller. Fault location at the midpoint is analyzed. The fault was cleared in the post-fault by removing the branch out at both sides. The black plot is the base case, the blue one is the ABC–TCSC controller, while the red one takes the proposed flower pollination algorithm (FPA)–TCSC controller.

After applying the fault at $t = 0.5$ s, the bus voltage declined as the fault time increases. The system was stable after clearing the fault by removing the short-circuit fault. With the ABC–TCSC controller added to the system, bus 4 voltage was improved to 0.66 p.u. during the faults, and, ultimately, its stability was enhanced after clearance of the fault compared to the base case. The figure shows that with the use of the proposed FPA–TCSC controller, the minimum voltage drop was 0.5268 p.u., and oscillation after the fault clearance was compressed better than the ABC–TCSC controller.

When compared to Fig. 9, the pre-fault stage of removing the branch from one side of the line and fully removing it from both sides of the line, as shown in Fig. 10, are the same. Only the post-fault stages are different from the rest. The plot shows that after the fault is cleared, the proposed FPA–TCSC controller provides better oscillation damping to achieve stability than the ABC–TCSC controller when compared to the base case.

Fig. 11 shows the convergence rate for the optimal tuning of both the FPA–TCSC parameter and ABC–TCSC parameter algorithm. Comparing the convergence curve of both the algorithms, the FPA reaches the optimal solution at the 93rd iteration, while the ABC reaches at the 190th iteration. This confirms that the FPA algorithm converges at a faster rate than the ABC algorithm.

2) Case B

In this simulation, the precise fault location, fault kind, and fault clearance time are taken into consideration. The three-phase fault was set on the transmission line L12–13 between two load buses, and the fault occurred at $t = 0.5$ s. The location of the fault was set at 10% away from the beginning of the branch L12–13 with a clearing time $t_c = 1.0$ s. After the simulation, among all the buses, bus 12 experienced a severe voltage drop of 0.045 p.u. It can be seen that both the proposed FPA–TCSC controller and ABC–TCSC controller were able to improve the voltage drop to 0.51 p.u. and 0.31 p.u., respectively, while making the system stable after the fault is cleared by removing the three-fault short-circuit fault as shown in Fig. 12. However, the suggested FPA-TCSC controller outperformed the ABC-TCSC controller because it could keep the bus stable at 1.0 pu. Fig. 13 shows that the fault is cleared by removing the branches at both sides. Both figures are the same when compared, which proves that when the fault occurs at that line, it can be cleared by either removing the short-circuit fault or by removing the branches out at both sides with the use of the proposed FPA–TCSC controller.

With a total time of 10 s, set for the simulation, a three-phase grounding short-circuit fault occurs at $t = 0.5$ s, with the fault located at the midpoint of the branch L12–13 and the fault duration is 0.5 s. The fault clearing is done by removing the short-circuit fault as shown in Fig. 14 or eliminating the faulty branch at both ends from the system as shown in Fig. 15. Both cases are the same, and the proposed FPA–TCSC controller played a critical role by maintaining the system stability at 1.0 p.u. while increasing the voltage drop from 0.157 p.u. to 0.461 p.u. when compared to the ABC–TCSC controller that had a voltage drop of 0.313 p.u. as shown in Fig. 14. As shown in Fig. 15, by eliminating the fault line, the voltage drop was 0.16 p.u. and was enhanced to 0.46 p.u. with the use of the proposed FPA–TCSC controller when compared to the ABC–TCSC controller, although both controllers were able to stabilize after the fault is cleared. In this case, firstly, during the post-fault scenario, the transient stability of the system does not depend on the mode of clearing the fault which is either by removing the three-phase fault or by removing the branch out from both sides of the buses using the proposed FPA–TCSC controller. Secondly, the proposed FPA–TCSC controller was able to maintain the bus to 1.0 p.u. for both figures.

B. IEEE 68-Bus System

1) Case C

To show the robustness of the proposed controllers on a large-scale system, the three-phase short-circuit fault is applied to the

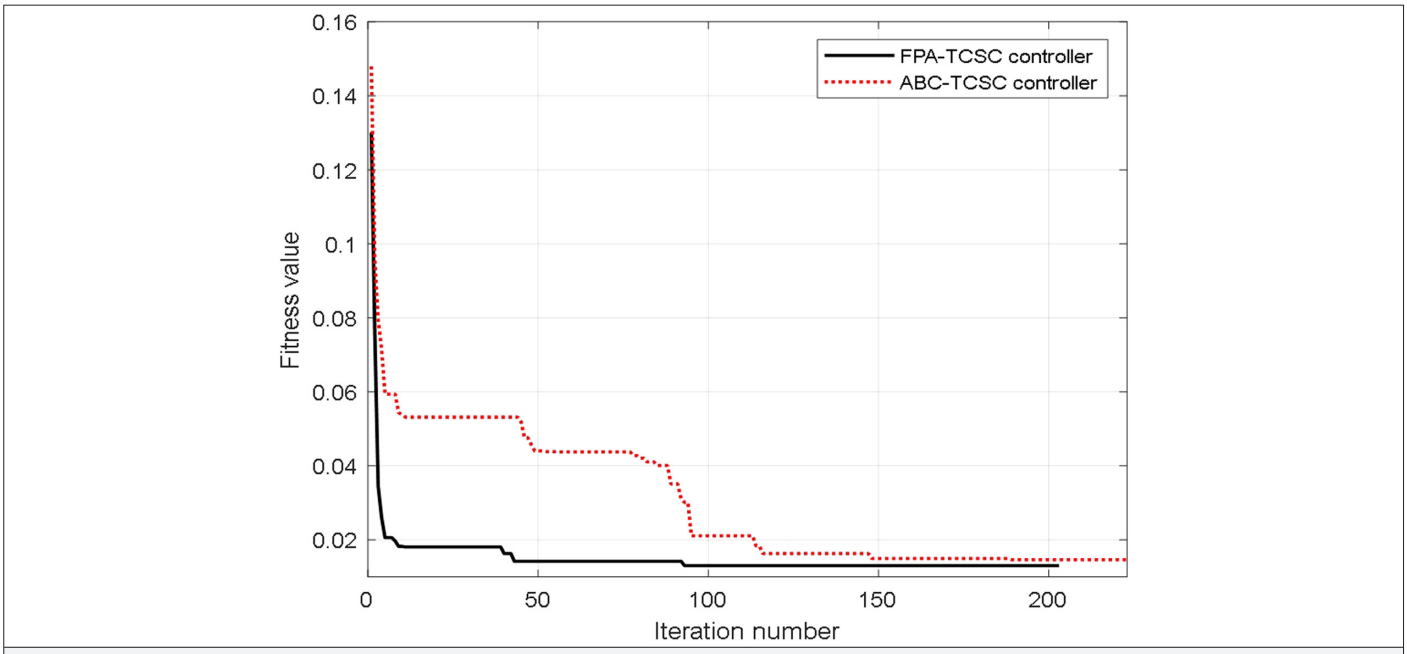

Fig. 11. Convergence curve of the flower pollination algorithm (FPA) and ABC. This plot shows the performance of the proposed FPA and ABC algorithm used to tune the parameters of the thyristor-controlled series capacitor (TCSC) controller.

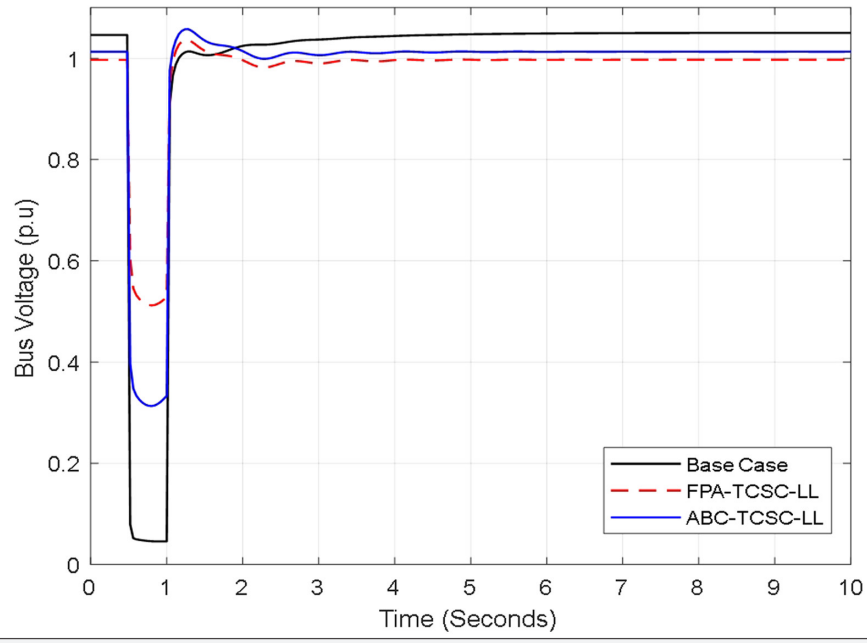

Fig. 12. Voltage magnitude after line fault (L12–13) at 10% distance with/without a thyristor-controlled series capacitor (TCSC) controller. Fault occurred between two loads and was cleared by removing the three-phase short circuit; the black line shows the plot of the base case and the blue line is the ABC–TCSC controller, while the red line takes the proposed flower pollination algorithm (FPA)–TCSC controller.

transmission line between two generator buses, and the results are compared to that of TCSC tuned using ABC. The fault is applied to line L02–25, which is located between generator bus 2 and generator bus 25. The distance of the line fault from bus 2 is 10%. From Fig. 16, in the pre-fault stage, all the buses were stable; after a three-phase fault occurred at line 02–25 at time $t=0.5$ s, bus 3 was severely unstable because of its closeness to the fault location with a voltage magnitude of 0 p.u. and after the fault is cleared by removing the short-circuit fault from the system after 0.5 s, it had a higher oscillation without being stable. It can be seen that with the use of ABC–TCSC controller, the speed of the oscillation was very lower than that of the base case but was not able to achieve stability; it comes with error. The use of the proposed FPA–TCSC controller was able to damp the oscillation successfully by achieving stability at the time of 1.6 s at 1.0 p.u.

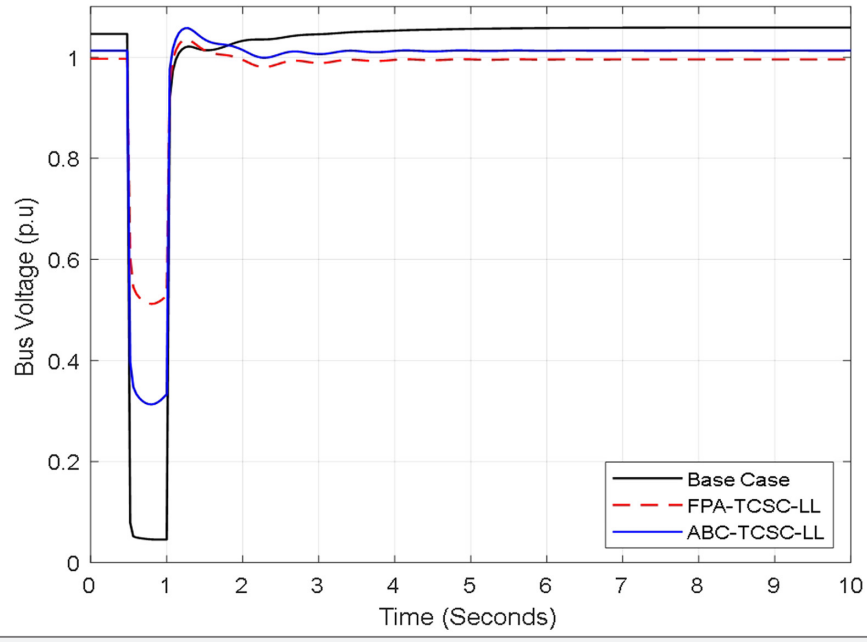

Fig. 13. Voltage magnitude after line fault (L12–13) at 10% distance with/without a thyristor-controlled series capacitor (TCSC) controller. Using the proposed flower pollination algorithm (FPA)–TCSC controller, as shown by the red line in the figure, stabilizes the system at 1.0 p.u. while enhancing the voltage drop during fault.

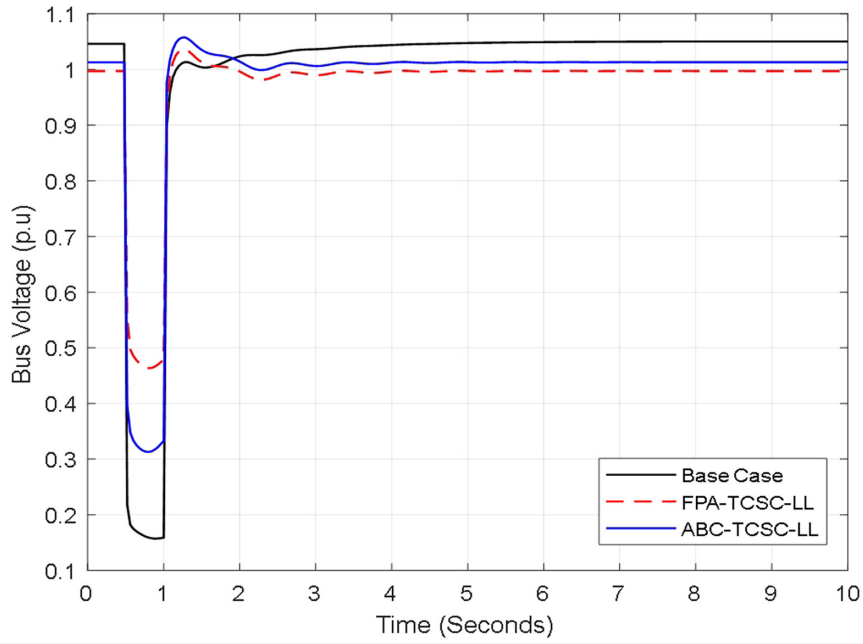

Fig. 14. Voltage magnitude after line fault (L12–13) at 50% distance with/without a thyristor-controlled series capacitor (TCSC) controller. Fault occurring between the midpoint of the load bus voltage does not drop lower compared to the 10% distance. The proposed flower pollination algorithm (FPA)–TCSC controller results are in red, ABC–TCSC controller in blue, and the base case is in black.

Fig. 17 displays the simulation output following the complete removal of the fault branch at both ends of the buses. The base case comes with a higher oscillation but better than when the fault was cleared by removing the short-circuit fault. The minimum voltage was 0 p.u. in the base case and the proposed FPA–TCSC controller damps out the oscillation by reaching stability with a minimum voltage of 0.5 p.u. which was better than the ABC–TCSC controller which only minimizes the oscillation amplitude with a minimum voltage of 0.36 p.u. compared to the base case.

The line fault was further increased from 0.1 pu to 0.5 pu, which is also the midpoint of line 02-25, to study the impact of fault

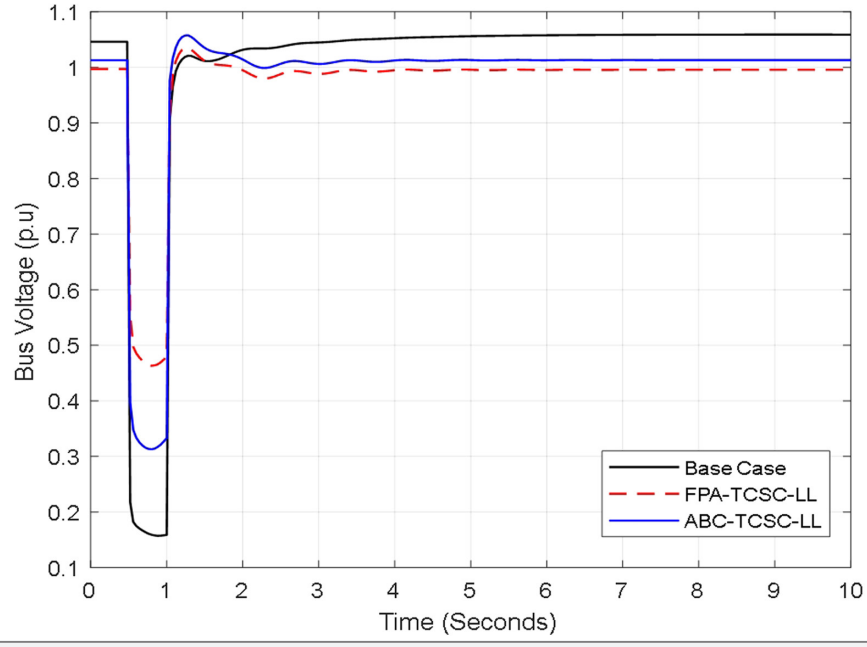

Fig. 15. Voltage magnitude after line fault (L12–13) at 50% distance with/without a thyristor-controlled series capacitor (TCSC) controller. With the fault cleared by eliminating the faulty branch at both ends of the system, the black plot shows the analysis in the base case, blue is the ABC–TCSC controller, while red takes the proposed FPA–TCSC controller.

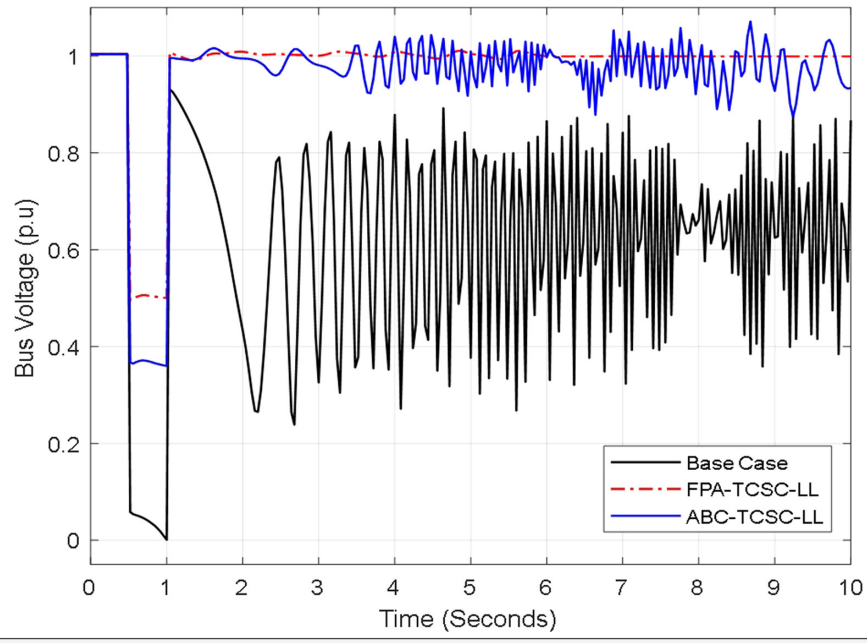

Fig. 16. Voltage magnitude after line fault (L02–25) at 10% distance with/without a thyristor-controlled series capacitor (TCSC). The plot consists of three lines: black shows the plot of the original system, while the blue line shows the ABC–TCSC controller; the red shows the system with the proposed flower pollination algorithm (FPA)–TCSC controller injection. The proposed FPA–TCSC controller stabilized the system after the fault was cleared.

distance on the system. From the simulation's results shown in Fig. 18, all buses were stable in the pre-fault stage. With the occurrence of the fault at time $t = 0.5$ s, bus 3 suffered the highest voltage drop with 0.32 p.u. in the base case because it is closer to the fault location, ABC–TCSC with 0.52 p.u., and the proposed FPA–TCSC controller with 0.6 p.u. The fault is cleared at time $t = 1.0$ s by removing the short-circuit fault from the system. It comes with few oscillations in the base case, and the use of ABC–TCSC controller cleared the oscillation compared to the base case but without reaching stability. Using the proposed FPA–TCSC controller damped the oscillation completely and reached stability at a simulation time of $t = 3.0$ s.

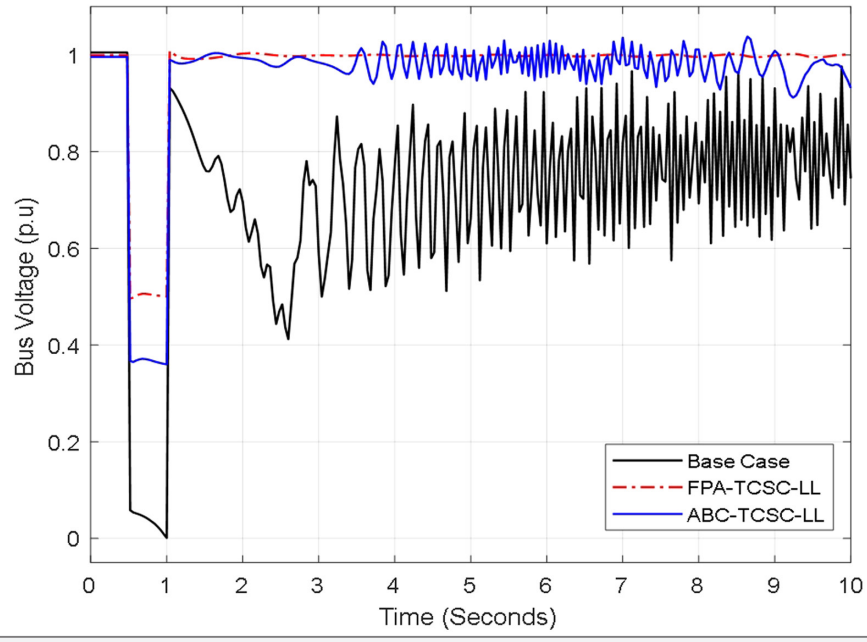

Fig. 17. Voltage magnitude after line fault (L02–25) at 10% distance with/without a thyristor-controlled series capacitor (TCSC) controller. With this graph, the fault was cleared by completely removing the branches from the end. Oscillation was still high in the base case shown in black, but using the proposed flower pollination algorithm (FPA)–TCSC controller made the system stable shown by a red line.

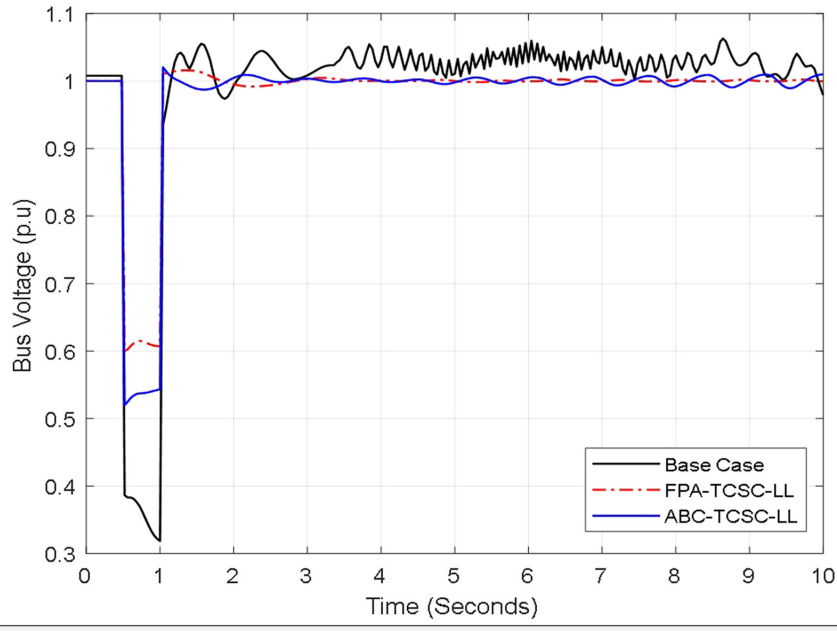

Fig. 18. Voltage magnitude after line fault (L02–25) at 50% distance with/without a thyristor-controlled series capacitor (TCSC) controller. Location of the fault was set at the midpoint of the line fault for the analysis. Using the proposed flower pollination algorithm (FPA) –TCSC controller, as shown in the red line, improved the voltage drop after the fault was cleared by removing the short-circuit fault compared to the base case in black color.

At the post-fault stage, the fault was cleared by eliminating the faulty branch on both sides of the buses after it had lasted 0.5 seconds at the midpoint between line 02-25 as shown in Fig. 19. The oscillation of the post-fault is very narrow as compared to Fig. 18 of the base case, with same applying to that of ABC–TCSC controller. The proposed FPA–TCSC controller damps the oscillation at a faster speed and achieves stability at a simulation time of $t = 3.0$ s.

2) Case D

In this case, to check the efficiency of the proposed controller, the line fault is then located between two load buses to determine the severity of the disturbances. The three-phase short-circuit fault is applied to line 15–16 between bus 15 and bus 16. The location of the fault was set at 10% away from the beginning of the branch L15–16. Fig. 20 shows the plot of the simulation when the fault happens on

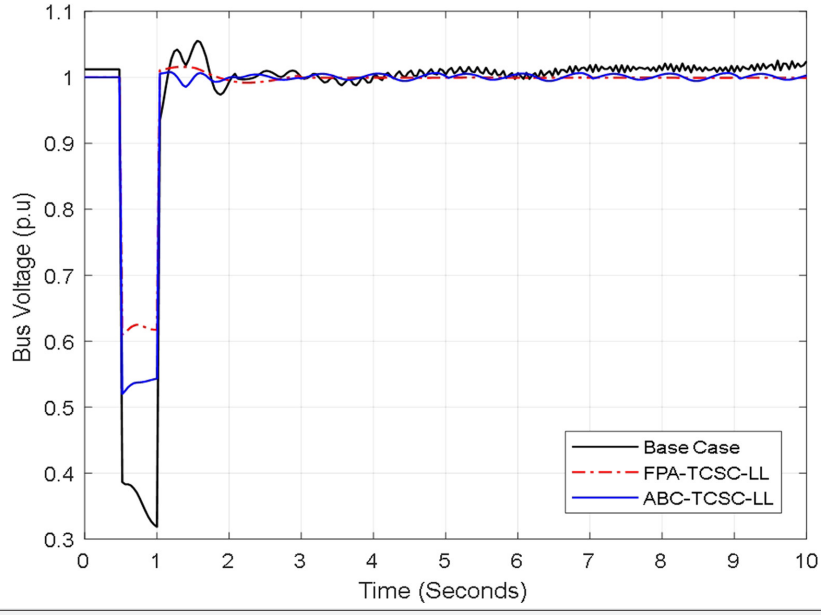

Fig. 19. Voltage magnitude after line fault (L02–25) at 50% distance with/without a thyristor-controlled series capacitor (TCSC) controller. Fault location at the midpoint is analyzed. The fault was cleared in the post-fault by removing the branch out at both sides. The black plot is the base case, blue is the ABC–TCSC controller, while red takes the proposed flower pollination algorithm (FPA)–TCSC controller.

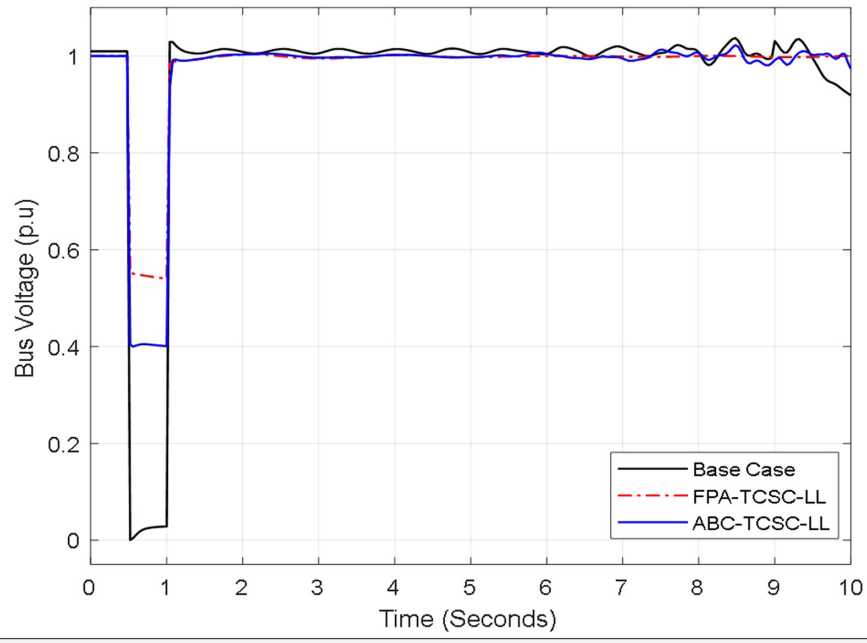

Fig. 20. Voltage magnitude after line fault (L15–16) at 10% distance with/without a thyristor-controlled series capacitor (TCSC) controller. Fault occurred between two loads and was cleared by removing the three-phase short circuit; the black line shows the plot of the base case and blue is the ABC–TCSC controller, while red takes the proposed flower pollination algorithm (FPA)–TCSC controller.

the line at $t = 0.5$ s, with bus 15 having the minimum voltage magnitude of 0.0 p.u. in the base case, and after the fault is cleared by removing the short-circuit fault from the system, it was not still stable with lesser amplitude oscillation. Use of the ABC–TCSC controller enhanced the voltage magnitude to 0.4 p.u. during the fault stage, and at $t = 1.0$ s, it was cleared with very little oscillation. The insertion of the proposed FPA–TCSC controller achieves the least voltage drop of 0.54 p.u. in the fault stage and was able to damp out the oscillation, with stability occurring at time $t = 3.4$ p.u.

After the fault clearance by removing the fault branch at both sides of the buses from the system, the simulation is plotted in Fig. 21, and the pre-fault and fault occurrence stages are the same in Fig. 20. By carefully comparing each figure, it can be noticed that the oscillation

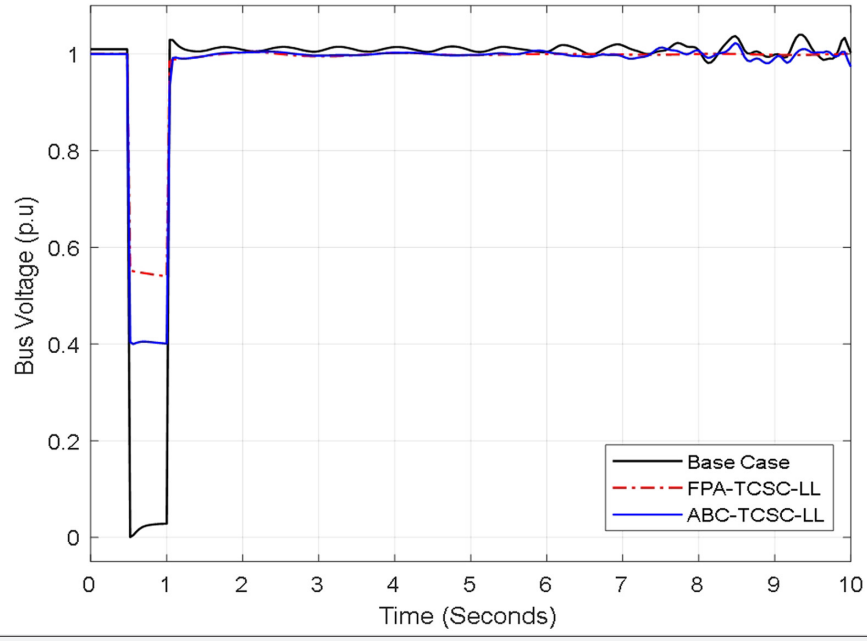

Fig. 21. Voltage magnitude after line fault (L15–16) at 10% distance with/without a thyristor-controlled series capacitor (TCSC) controller. Using the proposed flower pollination algorithm (FPA)–TCSC controller, as shown by the red line in the figure, stabilizes the system at 1.0 p.u. while enhancing the voltage drop during fault.

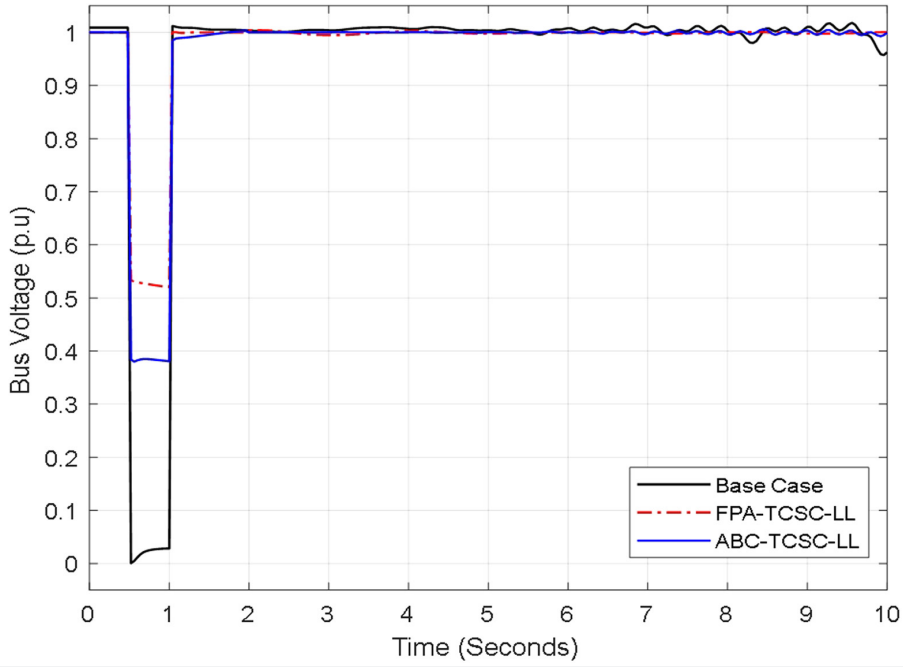

Fig. 22. Voltage magnitude after line fault (L15–16) at 50% distance with/without a thyristor-controlled series capacitor (TCSC) controller. Fault occurring between the midpoint of the load buses voltage does not drop lower compared to the 10% distance. The proposed flower pollination algorithm (FPA)–TCSC controller results are in red, ABC–TCSC controller in blue, and the base case is in black.

of both the base case and ABC–TCSC controller is narrow when the fault is cleared by removing the faulty line than by removing the three-phase fault. The proposed FPA–TCSC controller damped out the oscillation immediately after the fault clearance, reaching stability with no error.

Since the power system is negatively affected by fault distance, the line fault is further increased to the middle of lines 15 and 16, which is 0.5 pu away from line 15, and is simulated for a duration of 10 seconds, as shown in Fig. 22 and Fig. 23. In the initial stage, all buses were stable, and immediately after the line fault occurred at time

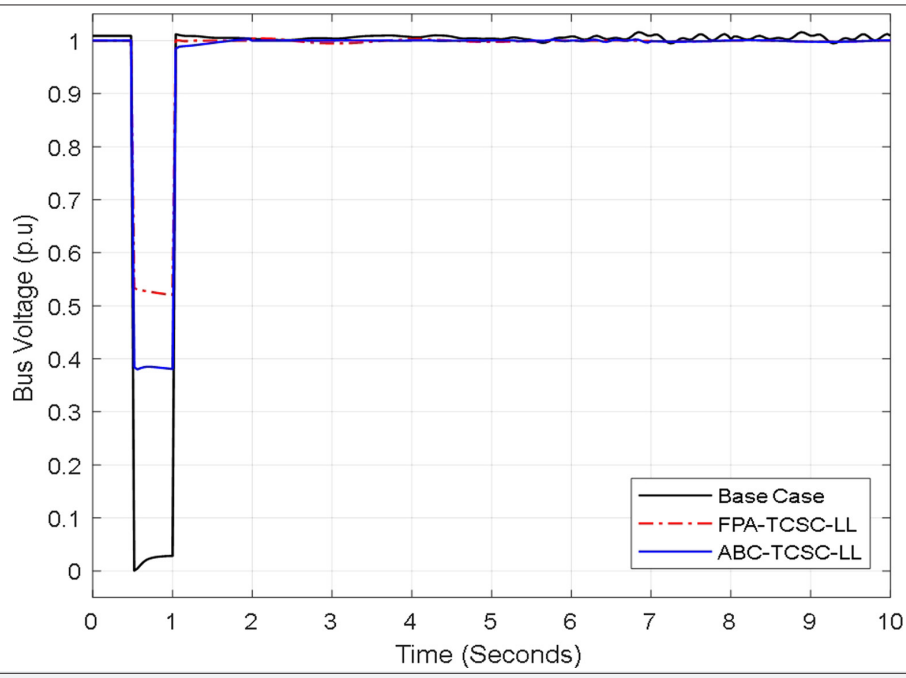

Fig. 23. Voltage magnitude after line fault (L15–16) at 50% distance with/without a thyristor-controlled series capacitor (TCSC) controller. With the fault cleared by eliminating the faulty branch at both ends of the system, the black plot shows the analysis in the base case and blue is the ABC–TCSC controller, while red takes the proposed flower pollination algorithm (FPA)–TCSC controller.

$t = 0.5$ s, all buses were unstable, but bus 15 was among the buses that had a lowest voltage magnitude drop of 0.0 p.u. which is shown in Fig. 22. The fault was cleared by removing the short-circuit fault from the system at $t = 1.0$ s. The base case had minor oscillations throughout the simulation with state error. It can be seen that both the proposed FPA–TCSC controller and ABC–TCSC controller were able to damp the oscillation and stabilize the system, but the proposed FPA–TCSC controller had a uniform stability immediately after the fault is cleared at 1.0 p.u. and with minimum voltage drop of 0.52 p.u. better than the ABC–TCSC controller with a minimum voltage magnitude of 0.38 p.u.

Fig. 23 represents the plot of simulation after the fault is cleared by removing the fault branch at both sides of the buses from the system. Fig. 9 is almost the same as Fig. 22, just that in the base case after the fault is cleared the oscillation at 9.7 s was narrower when compared to that of Fig. 22.

VII. CONCLUSION

This research focuses on improving the power system transient stability with the occurrence of three-phase fault to provide a safe and consistent power operation using the proposed FPA–TCSC lead–lag controller model. The proposed method was based on severity indices which can be used for large disturbances. The advantage of this index is that it can be used for offline mode and provides adequate information about the stability. The controller parameter tuning was set based on the ITAE value of the error and optimal location which are both solved as an optimization problem using the FPA. The effectiveness of the proposed model in improving the power system transient stability has been verified using the IEEE 14-bus system and IEEE 68-bus system through time-domain simulations under two different fault location and distances. It has been observed that when the fault is located between two generators buses at 10% fault location, the system was severely unstable with wider oscillation after the fault clearance with no controller. Also, simulation results show that the fault occurring on the transmission line between two load buses regains its stability when cleared either by removing the short-circuit fault or by the outage of the faulty line using the proposed FPA–TCSC controller. The test results illustrate the superiority of the proposed FPA-tuned TCSC controller when compared to that of the ABC-tuned controller. The overall conclusion is that the proposed FPA–TCSC controller model improved the power system's stability under severe disturbances and also increases the stability margin using the proposed method due to its accuracy and efficiency.

Peer-review: Externally peer-reviewed.

Author Contributions: Concept - D.O.A.; Design - D.O.A., A.A.M, H.H.; Supervision - G.I.R.; Analysis and/or Interpretation - D.O.A., A.A.M.; Literature Review - H.H.; Writing - D.O.A., A.A.M.; Critical Review - G.I.R.

Declaration of Interests: The authors have no conflicts of interest to declare.

Funding: The authors declared that this study has received no financial support.

REFERENCES

1. S. M. Hosseini, R. Abdollahi, and M. Karrari, "Inclusive design and implementation of online load angle measurement for real-time transient stability improvement of a synchronous generator in a smart grid," *IEEE Trans. Ind. Electron.*, vol. 65, no. 11, pp. 8966–8972, 2018. [CrossRef]
2. S. Raj, and B. Bhattacharyya, "Optimal placement of TCSC and SVC for reactive power planning using Whale optimization algorithm," *Swarm Evol. Comput.*, vol. 40, pp. 131–143, 2018. [CrossRef]
3. P. Kundur, "Definition and classification of power system stability IEEE/CIGRE joint task force on stability terms and definitions," *IEEE Trans. Power Syst.*, vol. 19, no. 3, pp. 1387–1401, 2004. [CrossRef]
4. T. Liu, Y. Liu, L. Xu, J. Liu, J. Mitra, and Y. Tian, "Non-parametric statistics-based predictor enabling online transient stability assessment," *IET Gener. Transm. Distrib.*, vol. 12, no. 21, pp. 5761–5769, 2018. [CrossRef]
5. P. M. Anderson, and A. A. Fouad, *Power System Control and Stability*. Chichester, UK: John Wiley & Sons, 2008.
6. T. Wang, J. Liu, S. Zhu, and Z. Wang, "Analytical on-line method of determining transient stability margin using protection information for asymmetric faults," *IET Gener. Transm. Distrib.*, vol. 14, no. 2, pp. 191–199, 2020. [CrossRef]
7. P. M. Anderson, *Analysis of Faulted Power Systems*. Chichester, UK: John Wiley & Sons, 1995.
8. J. Shi, B. Sullivan, M. Mazzola, B. Saravi, U. Adhikari, and T. Haupt, "A relaxation-based network decomposition algorithm for parallel transient stability simulation with improved convergence," *IEEE Trans. Parallel Distrib. Syst.*, vol. 29, no. 3, pp. 496–511, 2018. [CrossRef]
9. C. B. Saner, Y. Yaslan, and I. Genc, "An ensemble model for wide-area measurement-based transient stability assessment in Power Systems," *Electr. Eng.*, vol. 103, no. 6, pp. 2855–2869, 2021. [CrossRef]
10. R. Hassani, J. Mahseredjian, T. Tshibungu, and U. Karaagac, "Evaluation of time-domain and phasor-domain methods for power system transients," *Electr. Power Syst. Res.*, vol. 212, p. 108335, 2022. [CrossRef]
11. Y. Che, Z. Lv, J. Xu, J. Jia, and M. Li, "Direct method-based transient stability analysis for power electronics-dominated Power Systems," *Math. Probl. Eng.*, vol. 2020, pp. 1–9, 2020. [CrossRef]
12. J. Gao, B. Chaudhuri, and A. Astolfi, "A direct bounded control method for transient stability assessment," *IFAC PapersOnLine*, vol. 54, no. 19, pp. 294–301, 2021. [CrossRef]
13. A. A. Fouad, and V. Vittal, *Power System Transient Stability Analysis Using the Transient Energy Function Method*. London: Pearson Education, 1991.
14. T. L. Vu, and K. Turitsyn, "Lyapunov functions family approach to transient stability assessment," *IEEE Trans. Power Syst.*, vol. 31, no. 2, pp. 1269–1277, 2015. [CrossRef]
15. Y. Zhang, L. Wehenkel, P. Rousseaux, and M. Pavella, "SIME: A hybrid approach to fast transient stability assessment and contingency selection," *Int. J. Electr. Power Energy Syst.*, vol. 19, no. 3, pp. 195–208, 1997. [CrossRef]
16. B. Stott, "Power system dynamic response calculations," *Proc. IEEE*, vol. 67, no. 2, pp. 219–241, 1979. [CrossRef]
17. B. P. Soni, A. Saxena, V. Gupta, and S. L. Surana, "Assessment of transient stability through coherent machine identification by using least-square support vector machine," *Modell. Simul. Eng.*, vol. 2018, pp. 1–12, 2018. [CrossRef]
18. F. R. S. Sevilla, and L. Vanfretti, "A small-signal stability index for power system dynamic impact assessment using time-domain simulations." *IEEE PES Gen. Meeting*, 2014. [CrossRef]
19. N. I. A. Wahab, and A. Mohamed, "Area-based COI-referred rotor angle index for transient stability assessment and control of power systems," *Admin. Appl. Anal.*, vol. 2012, pp. 1–23, 2012. [CrossRef]
20. S. Niu, Z. Zhang, X. Ke, G. Zhang, C. Huo, and B. Qin, "Impact of renewable energy penetration rate on power system transient voltage stability," *Energy Rep.*, vol. 8, pp. 487–492, 2022. [CrossRef]
21. J. Pan, J. Fan, A. Dong, and Y. Li, "Random Vector Functional Link network optimized by Jaya algorithm for Transient Stability Assessment of Power Systems," *Math. Probl. Eng.*, vol. 2020, pp. 1–9, 2020.
22. M. M. Eladany, A. A. Eldesouky, and A. A. Sallam, "Power system transient stability: an algorithm for assessment and enhancement based on catastrophe theory and FACTS devices," *IEEE Access*, vol. 6, pp. 26424–26437, 2018. [CrossRef]
23. E. Ghahremani, and I. Kamwa, "Analysing the effects of different types of FACTS devices on the steady-state performance of the Hydro-Québec network," *IET Gener. Transm. Distrib.*, vol. 8, no. 2, pp. 233–249, 2014. [CrossRef]
24. M. Nandi, C. K. Shiva, and V. Mukherjee, "TCSC based automatic generation control of deregulated power system using quasi-oppositional harmony search algorithm," *Eng. Sci. Technol. An Int. J.*, vol. 20, no. 4, pp. 1380–1395, 2017. [CrossRef]

25. R. K. Singh, and N. K. Singh, "Power system transient stability improvement with facts controllers using SSSC-based controller," *Sustain. Energy Technol. Assess.*, vol. 53, p. 102664, 2022. [CrossRef]
26. M. A. M. Faroug, D. N. Rao, R. Samikannu, S. K. Venkatachary, and K. Senthilnathan, "Comparative analysis of controllers for stability enhancement for wind energy system with STATCOM in the grid connected environment," *Renew. Energy*, vol. 162, pp. 2408–2442, 2020. [CrossRef]
27. G. Yu, T. Lin, J. Zhang, Y. Tian, and X. Yang, "Coordination of PSS and facts damping controllers to improve small signal stability of large-scale power systems," *CSEE J. Power Energy Syst.*, 2019.
28. K. B. Meziane, R. Naoual, and I. Boumhidi, "Type-2 fuzzy logic based on PID controller for AGC of two-area with three source power system including advanced TCSC," *Procedia Comput. Sci.*, vol. 148, pp. 455–464, 2019. [CrossRef]
29. S. Ghaedi, S. Abazari, and G. Arab Markadeh, "Transient stability improvement of power system with UPFC control by using transient energy function and sliding mode observer based on locally measurable information," *Measurement*, vol. 183, p. 109842, 2021. [CrossRef]
30. A. Fathollahi, A. Kargar, and S. Yaser Derakhshandeh, "Enhancement of power system transient stability and voltage regulation performance with decentralized synergetic TCSC controller," *Int. J. Electr. Power Energy Syst.*, vol. 135, p. 107533, 2022. [CrossRef]
31. C. O. Maddela, and B. Subudhi, "Robust wide-area TCSC controller for damping enhancement of inter-area oscillations in an interconnected power system with actuator saturation," *Int. J. Electr. Power Energy Syst.*, vol. 105, pp. 478–487, 2019. [CrossRef]
32. N. A. Arzeha, M. W. Mustafa, and R. M. Idris, "Lead lag controller of TCSC optimized by bees algorithm for damping low frequency oscillation enhancement in SMIB," *Appl. Mech. Mater.*, vol. 781, pp. 374–378, 2015. [CrossRef]
33. S. C. Swain, S. Panda, and S. Mahapatra, "A multi-criteria optimization technique for SSSC based power oscillation damping controller design," *Ain Shams Eng. J.*, vol. 7, no. 2, pp. 553–565, 2016. [CrossRef]
34. M. Rahimi, M. Fotuhi-Firuzabad, and A. Karimi, "Short term voltage-based risk assessment by incorporating reactive power adequacy," *Ain Shams Eng. J.*, vol. 7, no. 1, pp. 131–141, 2016. [CrossRef]
35. S. Panda, "Differential evolutionary algorithm for TCSC-based controller design," *Simul. Modell. Pract. Theor.*, vol. 17, no. 10, pp. 1618–1634, 2009. [CrossRef]
36. Y. Nie, Y. Zhang, Y. Zhao, B. Fang, and L. Zhang, "Wide-area optimal damping control for power systems based on the ITAE criterion," *Int. J. Electr. Power Energy Syst.*, vol. 106, pp. 192–200, 2019. [CrossRef]
37. X.-S. Yang, "Flower pollination algorithm for global optimization," in *Unconventional Computation and Natural Computation*, 2012, pp. 240–249. [CrossRef]
38. X.-S. Yang, M. Karamanoglu, and X. He, "Multi-objective flower algorithm for optimization," *Procedia Comput. Sci.*, vol. 18, pp. 861–868, 2013. [CrossRef]

Ghamgeen I. Rashed was born in Sulaimani, Iraq. He received his B.Sc. degree in Electrical Engineering from Salahaadin University, Iraq, in 1995, M.Sc. degree from Sulaimani University, Iraq, in 2003, and Ph.D. degree in Power System and its Automation from the Huazhong University of Science and Technology (HUST), China, in 2008. He is currently an Assistant Professor with the School of Electrical Engineering, Wuhan University, China. His special research interests include AI and its application to power system, FACTS devices, especially TCSC, and its control.

Otuo-Acheampong Duku was born in Kumasi City, Ashanti Region, Ghana. He received his higher national diploma in Electrical and Electronic Engineering from Kumasi Technical University, in 2013, and B.Sc. degree in Electrical Engineering and Automation from China Three Gorges University, Yichang, China, in 2020. He is currently working toward the master's degree in Power System and Automation with the School of Electrical and Automation, Wuhan University, Wuhan, China. His current research interest is power system stability.

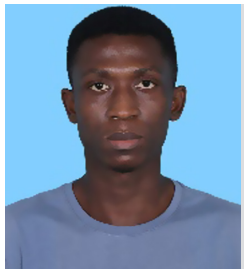

Amoh Mensah Akwasi received his bachelor's degree in Electrical Engineering and Automation from China Three Gorges University, China, in 2021. He is currently pursuing his master's degree in Electrical and Computer Engineering at South China University of Technology, China. He worked as an Assistant Electrical Engineer at Guangdong Jinlong Company Limited in Dongguan, China. His research interest includes power system and its automation.

Hussain Haider was born in Vehari, Pakistan. He received his B.S. in Electrical Engineering and Technology from the Institute of Southern Punjab, Multan, Pakistan, in 2015 and M.S degree in electrical Engineering from the Wuhan University, China, in 2020 and now he is a Ph.D scholar at the Smart Grid Research Institute at School of Electrical Engineering and Automation, Wuhan University, Hubei, China. His special research interest includes FACTS devices, in particular, TCSC, UPFC, and its control; power transmission networks; smart grids; demand side management, and internet of things.